An investigation of damage healing in high temperature compressive forming process

Zhou, Wenbin; Afshan, Shireen; Lin, Jianguo

Published in:
Procedia Manufacturing

DOI:
10.1016/j.promfg.2020.08.108

Publication date:
2020

Available online at www.sciencedirect.com

ScienceDirect

Procedia Manufacturing 50 (2020) 602–608

Procedia MANUFACTURING

www.elsevier.com/locate/procedia

18th International Conference Metal Forming 2020

An investigation of damage healing in high temperature compressive forming process

Wenbin Zhou*, Shireen Afshan, Jianguo Lin

Department of Mechanical Engineering, Imperial College London, London SW7 2AZ, UK

* Corresponding author. *E-mail address:* w.zhou15@imperial.ac.uk

Abstract

Damage healing in steel parts enables them to be reused again without going through the conventional metal recycling/remelting process, thus damage healing is a process with potential for reclaiming products while causing less environmental damage, that is, improving resource efficiency. In this paper, damage healing of a porous free cutting steel during a hot flat rolling process has been investigated. A UMAT subroutine incorporating damage healing models has been utilised which includes two stages: void closure and diffusion bonding. The developed UMAT subroutine captures evolution of void volume fraction (*vvf*) as a result of plastic compression, to model the void closure process and predict the subsequent healing time. Effects of roll gap geometry factor (*RGF*), initial porosity size (void volume fraction) on porosity elimination during rolling have been investigated.

Keywords: Damage healing; High temperature; Compressive forming; Hot rolling; Void closure; Diffusion bonding

1. Introduction

Mechanical properties of materials can be undermined by the existence of micro-voids and micro-structural damage. Accumulation of micro-damage leads to micro-crack initiation and propagation which undermine structural integrity and often, eventual fracture [1]. Thus the service life of a structural part can be significantly reduced.

Although robust, high quality products can be produced using well-designed manufacturing processes, in some cases creation of micro-damage is unavoidable. Nevertheless, if damage elimination/healing is incorporated in a process, material damage can be reduced or eliminated and the full inherent properties of a product can be realised.

Healing has been widely used in many different fields, including recovery of biomaterials [2,3], composites and polymers [4,5], and concrete [6,7]. Healing in metals has mostly been undertaken at elevated temperature (e.g. at 0.7-0.9 times the metal melting temperature). For powder metallurgy processing this entails liquid phase or solid state bonding across powder interfaces through metallic mass transfer [8]. In addition to the above healing methods, for various metal alloys diffusion bonding has also been used. Diffusion bonding is a process where two solid surfaces are joined at elevated temperature and pressure. Bonding temperature normally is a value ranging between 0.5-0.8 times absolute melting point temperature of the work-piece alloy. Partially or completely recovered mechanical properties of damaged metal materials can be achieved by sintering or diffusion bonding/healing techniques and damaged steel parts in built structures seem suitable items for application of the techniques with potentially rewarding outcomes.

A schematic of healing of metals by a compressive forming process at high temperature, is shown in Fig. 1. Damage healing in metals is envisaged as a two-stage process. In the first stage under the action of compression between opposing dies, slits (cracks) are formed by closing of existing voids. However, the surfaces of the cracks have not been

10.1016/j.promfg.2020.08.108

completely bonded (the interfaces consist of an array of voids with irregular shapes) and have little adhesion under tension. In the second stage, under continued compression, diffusion occurs across crack interfaces which become metallurgically bonded.

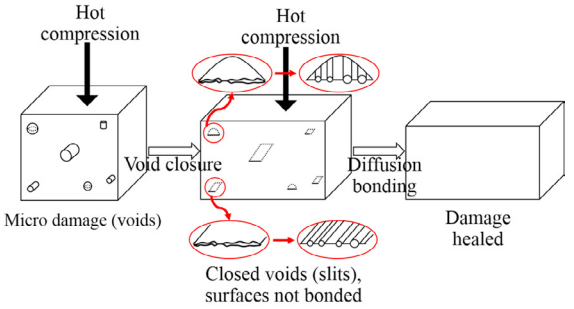

Fig. 1. Damage healing in hot compressive forming process.

Effects of work-piece thickness reduction, die geometry and deformation rate on void closure behaviour during hot rolling or forging have been studied [9,10]. It has been found that normally, a large value of the ratio of roll radius to work-piece thickness or large reduction in work-piece thickness will accelerate the void closure process, and large void fractions are harder to be removed than small ones. Dudra and Young-Taek [9] investigated the influence of geometry of die (FML, double V, and flat) and billet (round and square) on void closure during forging. V-shaped dies were found to favour void closure process, due to the greatest effective strain and hydrostatic stress being produced. Also, void closure in a round billet occurred at a greater reduction but at lower press load than that in a square billet. Effects of pressure, temperature and time have also been studied [11,12]. Usually voids close more quickly and easily when plastic deformation occurs together with significant hydrostatic pressure. Wang et al. [13] showed that void closure starts when the hydrostatic pressure reaches a certain value and speeds up at elevated temperatures, while the degree of healing is also affected by compressive pressure holding time. The subsequent healing process is affected by parameters such as pressure, temperature and duration of load-temperature application. Normally, an increase in the hydrostatic compressive stress leads to substantial reduction in time to complete healing. Temperature accelerates the healing process significantly and healing time is shortened by increasing temperature.

Several damage healing models exist and although they contain similar assumed mechanisms each leads to different predicted healing rates as different details of bonding mechanisms, void geometries, void positions and operations (series and parallel), have been adopted. Different mechanisms have been proposed for damage healing models. Some [14-18] were derived from void growth models, where void shrinkage was regarded as negative void growth. Some other models [19,20] were obtained from powder sintering models.

Different void geometries have been studied for the modelling of damage healing. It is popularly assumed that surface diffusion is fast enough to keep the void shape spherical [21-23]. In some models contact surfaces are considered to be triangular ridges which gradually shrink into channels with circular cross sections [19]. Wang and Li [24] suggested that a grain-boundary void changes its shape to a spheroid as atoms migrate along the void surface and grain-boundary. In some other models a cylindrical shape void geometry has been assumed [25,26]. A cylindrical pipe shape with lenticular and rhombic cross-section has been investigated. Gue and Ridly [27] considered a lenticular initial void shape. Takahashi [28] assumed a rhombic geometry as the initial void shape and a lenticular geometry during diffusion.

Healing models have also been developed for different void positions, such as, voids within a grain boundary [23,29] and voids on a grain boundary [22,25,29]. The final shape of a void within a grain depends on the balance between the elastic energy stored in the solid and the surface energy. However, for a grain boundary void this is determined by the difference in elastic energy, surface and grain boundary energies [24]. The primary healing mechanisms for voids within a grain boundary are, lattice diffusion and surface diffusion. For spherical voids, lattice diffusion is the dominant mechanism as surface diffusion is fast and can be ignored [29].

Series and parallel operations have been considered for modelling damage healing. An examination of models for void shrinkage on a bond interface shows that parallel operations have usually been considered. In parallel operations all possible bonding mechanisms act independently in such a way that their contribution to bonding can be added together to obtain the total amount of bonding. In void growth models it is assumed that interface and surface diffusion occur in series. In series operations, depending on the values of surface diffusion and grain boundary diffusion coefficients (D_s and D_{gb}, respectively), the rate controlling mechanism can be identified. If $D_s \gg D_{gb}$, surface diffusion is much faster than grain boundary diffusion. This means that grain boundary diffusion is rate controlling and surface diffusion can be ignored in calculating the healing time. However, if $D_{gb} \gg D_s$ (grain boundary diffusion is much faster than surface diffusion), surface diffusion is rate controlling, resulting in a convex surface at the void tip and the moving of the sink point towards the void surface [28].

In this paper, firstly the damage mechanisms and evolution characteristics are introduced. Then, the damage healing of a porous free cutting steel during a hot flat rolling process has been studied using a UMAT subroutine incorporating damage healing models. Effects of roll gap geometry factor (*RGF*) and initial porosity size (void volume fraction) on porosity elimination during rolling have been explored.

2. Damage mechanisms and evolution

Material failure is a result of heterogeneous micro processes which undermine the mechanical properties of the material. A solid is considered as damaged after losing some of its microstructural bonds. Failure occurs more easily for materials with micro-damage (process-induced or appear during loading), including distributed microscopic cavities, voids, or micro-cracks [30]. Damage healing can be regarded as a reversed damage evolution process, therefore it is useful to

briefly elucidate damage mechanisms before studying damage healing. The process of ductile damage in metals is of greatest interest here. Ductile damage evolves in a multistep process involving several interactive and concurrent mechanisms – void nucleation, growth, and coalescence, progress simultaneously but at different rates (Fig. 2).

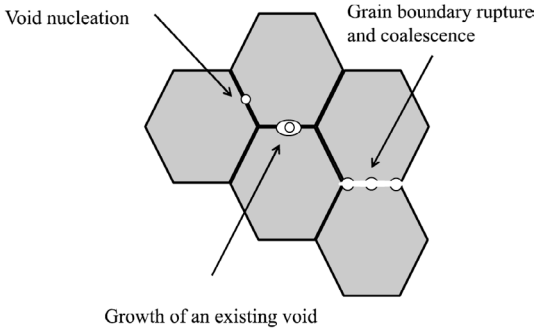

Fig. 2. Damage mechanisms.

Nucleation: In structural alloys there exist impurities such as second-phase particles and inclusions. Cavities nucleate as a result of fracture of these particles or decohesion of the particle-matrix interface, during deformation [31]. Volume fraction and size of particles highly affect void nucleation; greater particle volume fractions and particle sizes speed up the nucleation process. This is due to increased interactions between secondary plastic zones of particles at high particle volume fractions, also for large particles, the number of surrounding dislocations increases, making the plastic relaxation easier [31].

Growth: Nucleated cavities will grow with increase of plastic deformation. The growth of an isolated cylindrical [32] or spherical void [33] for a certain deformation state has been investigated, indicating that void growth rate increases exponentially with stress triaxiality. In addition, constitutive equations for ductile materials containing voids have been established using homogenization theory [16].

Coalescence: Micro-void coalescence occurs when a certain critical condition for local plastic instability is fulfilled, that is, the matrix between neighbouring voids is sufficiently thinned down. This can usually be seen during necking. Coalescence is normally a localised and non-homogeneous deformation process. Prediction models for the onset and development of coalescence have been proposed. Void coalescence has been modelled by a heuristic approach which decreases the stress to zero or accelerates the void growth to the situation of complete loss of the stress carrying capacity. A proposed criterion for coalescence onset, is that when void volume fraction, vvf, which is a material-dependent constant, reaches a critical value vvf_c [34]. Nevertheless, it is also argued that vvf_c is a value that varies with stress state and can be obtained from micromechanically based models [35].

3. Damage healing modelling in a hot rolling process

Fig. 3 illustrates flat rolling geometries, for which start and end work-piece cross-sections are rectangular. One important parameter affecting the rolling force is the roll gap geometry/shape factor (RGF). The stress regime in the work-piece between the rollers is highly affected by this parameter [36]. The RGF is defined as, $RGF = L/H_m$, where L and H_m are obtained by $L \sim (R_r(H_1\text{-}H_2))^{0.5}$ and $H_m = (H_1+H_2)/2$. Here R_r is the rollers radius, L is the projected arc of contact between roll and work-piece, H_1 and H_2 are work-piece thickness before and after passing through the rollers, respectively [36].

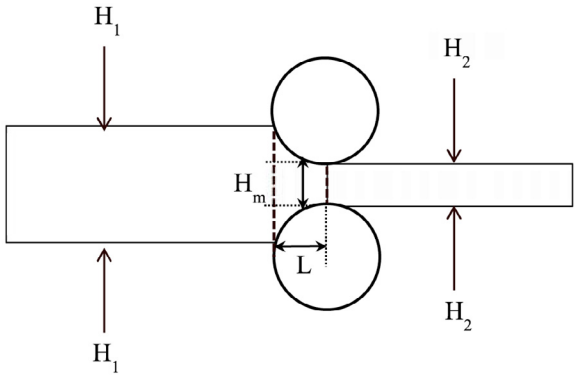

Fig. 3. Schematic illustration of geometries in rolling.

The porosity elimination process during hot flat rolling has been investigated, using a three-dimensional model of two rolls and a billet; a schematic of the billet is shown in Fig. 4a. The billet has a cross sectional area of 324 cm^2 (18×18 cm) and length of 49.649 cm. Since the billet has a symmetric geometry, only a quarter of the billet has been modelled to save computational time. The rolls have radius of 34.75 cm and H_m/L= 3.5.

In Fig. 4a, plane ‘acge’ is symmetric relative to the x axis ($U_x = UR_y = UR_z = 0$) and plane ’cdhg’ is symmetric relative to the y axis ($U_y = UR_x = UR_z = 0$). The billet has a velocity of 4.49 cms^{-1} in z direction. The velocity of the rollers in x, y, z direction is zero. The angular velocity of the rollers are defined as -0.1288 rad/s and 0.1288 rad/s. The rolls are 3D analytical rigid bodies and are in contact (surface-to-surface contact) with the billet. A ‘tangential behaviour’ for the contact surfaces was defined using the penalty method. The friction coefficient between the roll and the steel work-piece was taken to be 0.3 (the reduction in the product thickness occurs only if the shear frictional stress is greater than a minimum value). Unless otherwise stated, the default values in ABAQUS/Standard for surface to surface contact were used for all other parameters [37].

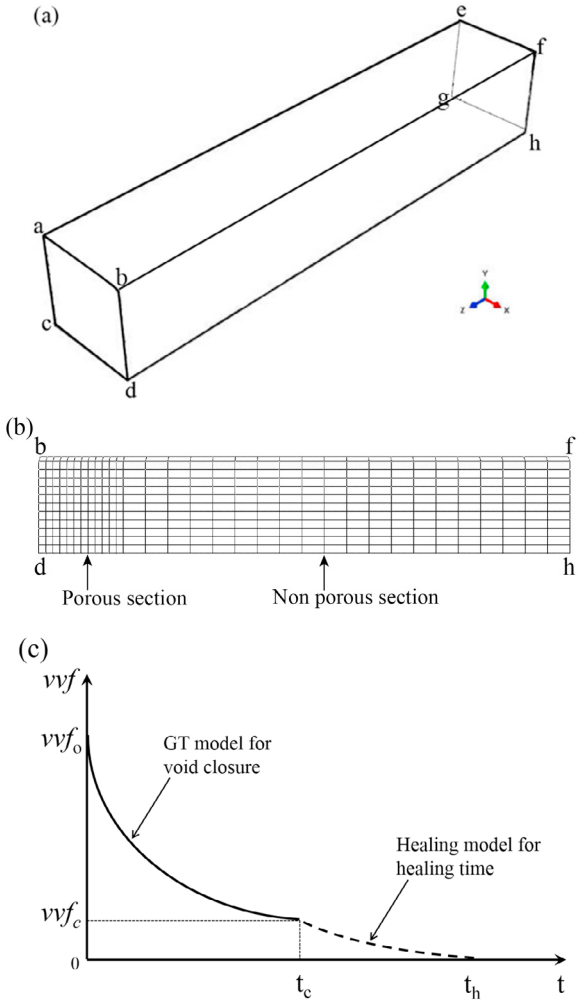

Fig. 4. Illustration of the billet: (a) geometry model; (b) FE model; (c) variation of *vvf* with time for GT model and healing model.

To study porosity elimination in the work-piece, only a section of the billet has been given porous material properties, as shown in Fig. 4b. A UMAT subroutine has been developed for analysing material porosity elimination comprising the two stages of void closure and healing [38,39]. The developed UMAT subroutine uses the Gurson–Tvergaard (GT) model under reverse loading to predict void closure [38]. As a result of plastic compression the void volume fraction of the material, *vvf*, reduces to vvf_c, the void volume fraction at which healing is initiated. Further, the model proposed by Pilling [26] was incorporated in the UMAT subroutine to predict healing time [39]. The elimination of voids involves three processes. These processes involve the collapse of the supporting contact area by plastic deformation and creep, diffusion of atoms from grain boundaries to the voids via both volume and interfacial paths and surface diffusion or transfer of mass along the void surface. The reverse GT and healing models have previously been described in detail in [38,39], a schematic illustration of evolution of void volume fraction *vvf* during healing is shown in Fig. 4c, where t_c is the time at which the void closes, t_h is the time required for healing.

The developed UMAT subroutine has been applied to the porous section and a finer mesh has been used. The FE model represents only one stand in a roughing stage. Fig. 4b represents the block partitioning and the applied mesh. The work-piece consists of a total of 3904 elements with 1464 elements in the porous region. A mesh with 8-node linear brick, reduced integration elements (C3D8R in ABAQUS terminology) was used.

The non-porous section of the work-piece was modelled using a von Mises yield surface equivalent to the GT model with $vvf = 0$. The initial void volume fraction of the porous section was taken to be $vvf_o = 0.006$ and vvf_c of 0.003 was assumed. The experimentally obtained material properties for free cutting steel (FCS) at 900 °C and $\dot{\varepsilon} = 0.1$ [40] were used. The calibrated fitting parameters of the GT model, $q_1 = 2.0$, $q_2 = 1.25$ and $q_3 = 4.0$ under these values of void volume fraction ($vvf_o = 0.006$ and $vvf_c = 0.003$) were obtained for an average triaxiality, $T = -0.5$ [38].

4. Results and discussion

4.1. Void elimination during rolling

Fig. 5a shows the pressure distribution and evolution throughout the work-piece as it is compressed through the rollers. The compression may be sufficient at some positions in the work-piece and therefore closure and healing may occur in some parts. However, at some positions, the amount of compression and plastic deformation may not be enough for a closure state to be reached and healing may never occur. In Fig. 5b some of the elements have reached the closure state ($vvf = vvf_c = 0.003$) and started to heal. These elements are shown in red. As the work-piece is rolled more elements experience compression and the number of these element (shown in red) increase.

It should be noted that in Fig. 5b, although some elements (represented in red) have reached the closure state and have started to heal, more time is required for these elements to heal completely ($vvf = 0$). Since the stress state in the work-piece is non-uniform, healing times are different for each element. To have an approximate estimation of predicted healing time for the studied case, three random elements were selected from the model as shown in Fig. 6a. The change in *vvf* with time during healing for these elements is shown in Fig. 6b. Predicted healing times of 19.1 s, 23.6 s and 20.4 s for element A, B and C, respectively, can be seen. The average healing time for all closed elements (red elements in Fig. 5b) is 18.1s.

4.2. Effect of roll gap geometry factor on porosity closure

As mentioned in section 3, the stress regime within the work-piece between the rolls is highly affected by roll gap geometry/shape factor (*RGF*). For $H_m/L > 4.8$ (where $H_m/L = RGF^{-1}$) all principal stresses are tensile, therefore representing a regime of tensile triaxiality. For $1.8 < H_m/L < 4.8$, the vertical principal stress is compressive, but all the other stresses are tensile. For $1 < H_m/L < 1.8$, the hydrostatic stress becomes compressive [36]. Here the porosity closure has been

investigated for a range of H_m/L values, with the understanding that greater closure will enable greater healing; the trend with H_m/L can be understood without simulating healing. To compare the closure extent for different H_m/L cases, closure percentage (defined as the ratio of number of closed elements to total element number) has been obtained for H_m/L values of 2.5, 3.5, 4.5, 6.5 and 8.

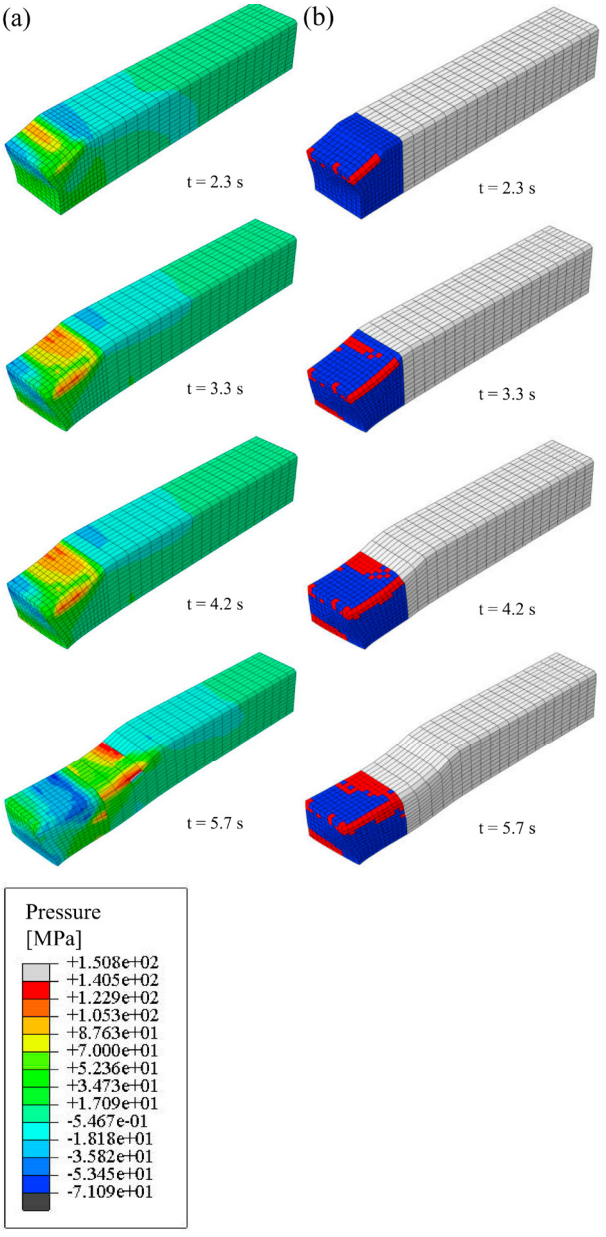

Fig. 5. (a) Pressure distribution along the billet (positive values represent compression); (b) void elimination process (red represents elements that have reached the closure state and started to heal).

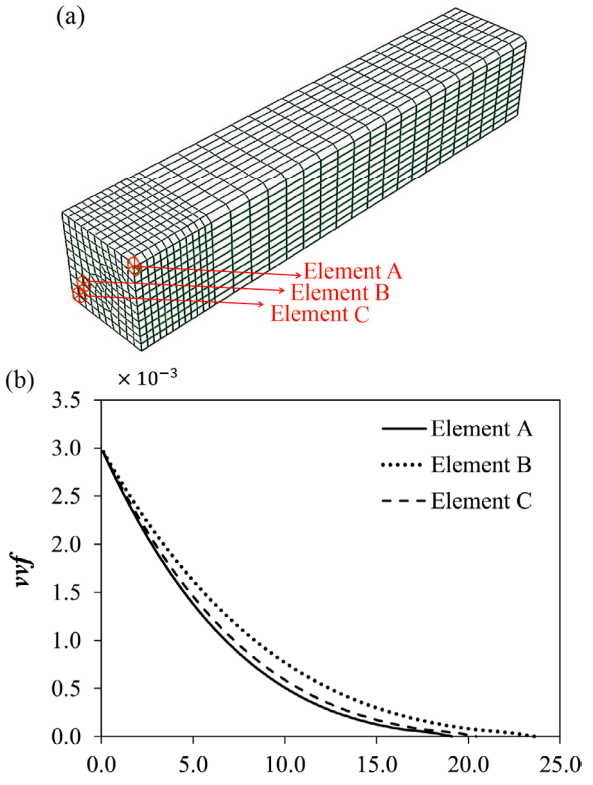

Fig. 6. (a) Elements selected for study of healing time; (b) *vvf* versus time for element A, B, and C.

As illustrated in Fig. 7, closure percentage (% Closure) increases as H_m/L decreases. Lower closure percentage is obtained for H_m/L values of 6.5 and 8. This is because all principal stresses and stress triaxiality are tensile for these cases. The closure percentage is higher for H_m/L values of 2.5 and 3.5. As mentioned before, for $1.8 < H_m/L < 4.8$, the vertical principal stress becomes compressive, therefore porosity closure will be promoted at a greater rate. It is worth mentioning that the value of vvf_c is an assumption here; in real cases the value of vvf_c might be smaller and therefore the closure percentage values could be different.

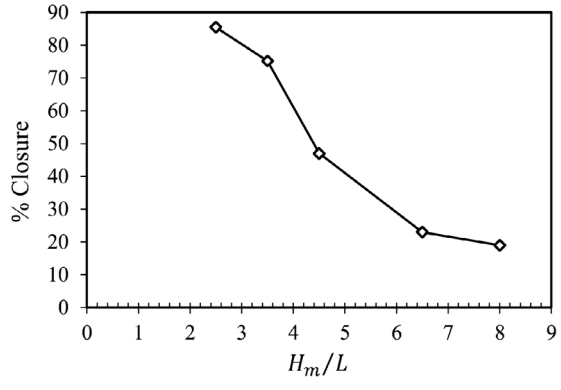

Fig. 7. Closure percentage obtained during rolling for different H_m/L values.

4.3. Effect of initial porosity size on porosity closure

The porosity elimination in rolling is highly affected by the amount of initial porosity present in the work-piece, or in other words, the initial void volume fraction (vvf_o). Higher values of vvf_o, require larger compression (larger reduction in work-piece thickness) and also longer times. **Fig. 8** compares the percentage of closure of a billet with initial porosity values of $vvf_o = 0.02$ and $vvf_o = 0.03$ rolled under the same conditions. As is evident from this figure, for initial void volume fraction of $vvf_o = 0.02$, the amount of compression has been sufficient to produce a relatively high closure percentage of around 91%, whereas for a slightly higher initial porosity of $vvf_o = 0.03$, the closure percentage is relatively smaller (~19 %).

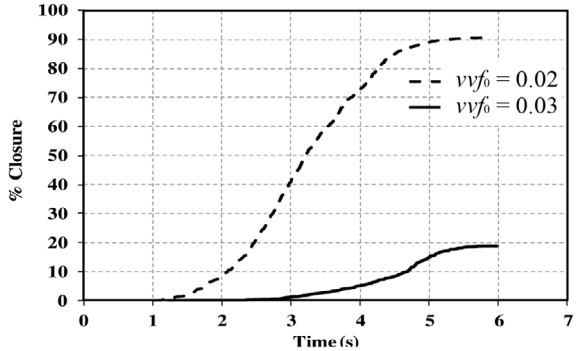

Fig. 8. Closure percentage versus time for two different values of initial porosity vvf_o.

5. Conclusions

The developed UMAT subroutine incorporating damage healing models has been applied to model the damage healing of a steel work-piece during rolling. The effect of roll gap geometry/shape factor ($RGF = L/H_m$) on porosity elimination during rolling was investigated. Generally, damage healing increases as H_m/L decreases. For $H_m/L > 4.8$ all principal stresses are tensile, representing a regime of tensile triaxiality which leads to a lower amount of healing compared to cases of $1.8 < H_m/L < 4.8$, when the vertical principal stress becomes compressive and porosity closure occurs. The porosity closure will be promoted at a greater rate for $1 < H_m/L < 1.8$ as a result of the compressive hydrostatic stress in this case. The effect of initial void volume fraction on porosity elimination in rolling was also investigated. It was observed that for larger initial void volume (vvf_o) fractions the amount of damage healing was lower. This was due to the amount of compression for larger values of vvf_o not being sufficient at some locations in the work piece, to reach the closure state.

Acknowledgements

The financial support from EPSRC (grant No: EP/S019111/1) is greatly appreciated.

References

[1] Lin J, Liu Y, Dean TA. A review on damage mechanisms, models and calibration methods under various deformation conditions. International Journal of damage mechanics 2005;14:299-319.
[2] Fratzl P, Weinkamer R. Hierarchical structure and repair of bone: deformation, remodelling, healing. In: Van der Zwaag S, editor. Self healing materials. Dordrecht: Springer; 2007. p. 323-35.
[3] Vermolen F, Rossum M, Perez E, Adam J. Modeling of self healing of skin tissue. In: Van der Zwaag S, editor. Self healing materials. Dordrecht: Springer; 2007. p. 337-63.
[4] Blaiszik BJ, Kramer SLB, Olugebefola SC, Moore JS, Sottos NR, White SR. Self-healing polymers and composites. Annu. Rev. Mater. Res 2010;40:179-211.
[5] Wool RP, O'connor KM. A theory crack healing in polymers. J Appl Phys 1981;52:5953-63.
[6] Li VC, Yang E. Self healing in concrete materials. In: Van der Zwaag S, editor. Self healing materials. Dordrecht: Springer; 2007. p. 161-93.
[7] Reinhardt HW, Jooss M. Permeability and self-healing of cracked concrete as a function of temperature and crack width. Cem Concr Res 2003;33:981-5.
[8] Lumley RN, Polmear IJ. Advances in self-healing of metals. Proceedings of the first international conference on self healing materials. The Netherlands: Springer; 2007. p. 219-54.
[9] Dudra SP, Young-Taek I. Analysis of void closure in open-die forging. Int J Mach Tools Manuf 1990;30:65-75.
[10] Park CY, Yang DY. Modelling of void crushing for large-ingot hot forging. J Mater Process Technol 1997;67:195-200.
[11] Han J, Zhao G, Cao Q. Internal crack recovery of 20MnMo steel. Sci China Ser E Technol Sci 1997;40:164-9.
[12] Wei D, Han J, Jiang ZY, Lu C, Tieu AK. A study on crack healing in 1045 steel. J Mater Process Technol 2006;177:233-7.
[13] Wang A, Thomson PF, Hodgson PD. A study of pore closure and welding in hot rolling process. J Mater Process Technol 1996;60:95-102.
[14] Guo ZX, Ridley N. Modelling of diffusion bonding of metals. Mater Sci Technol 1987;3:945-53.
[15] Hancock JW. Creep cavitation without a vacancy flux. Metal Sci 1976;10:319-25.
[16] Gurson AL. Continuum theory of ductile rupture by void nucleation and growth: part I— yield criteria and flow rules for porous ductile media. J Eng Mater Technol Trans ASME 1977;99:2-15.
[17] Tvergaard V. Influence of voids on shear band instabilities under plane strain conditions. Int J Fract 1981;17:389-407.
[18] Tvergaard V. On localization in ductile materials containing spherical voids. Int J Fract 1982;18:237-52.
[19] Derby B, Wallach ER. Theoretical model for diffusion bonding. Metal Sci 1982;16:49-56.
[20] Hill A, Wallach ER. Modelling solid-state diffusion bonding. Acta Metall 1989;37:2425-37.
[21] Speight MV, Beere W. Vacancy potential and void growth on grain boundaries. Metal Sci 1975;9:190-1.
[22] Beere W, Speight MV. Creep cavitation by vacancy diffusion in plastically deforming solid. Metal Sci, 1978;12:172-6.
[23] Sun J. A model for shrinkage of a spherical void in the center of a grain: Influence of lattice diffusion. J Mater Eng Perform 2002;11:322-31.
[24] Wang H, Li Z. The three-dimensional analysis for diffusive shrinkage of a grain-boundary void in stressed solid. J Mater Sci 2004;39:3425-32.
[25] Chen IW, Argon AS. Diffusive growth of grain-boundary cavities. Acta Metall 1981;29:1759-68.
[26] Pilling J, Ridely N. Solid state bonding of superplastic AA 7475. Mater Sci Technol 1987;3:353-9.
[27] Guo ZX, Ridely N.. Modelling of diffusion bonding of metals. Mater Sci Technol 1987;3:945-53.
[28] Takahashi Y, Inoue K.. Recent void shrinkage models and their applicability to diffusion bonding. Mater Sci Technol 1992;8:953-64.
[29] Wang H, Li Z.. Diffusive shrinkage of a void within a grian of a stressed polycrystal. J Mech Phys Solids 2003;51:961-76.
[30] Zhang R, He R, Zhou W, Wang Y, Fang D. Design and fabrication of porous ZrO_2/(ZrO_2+Ni) sandwich ceramics with low thermal conductivity and high strength. Mater Des 2014; 62:1-6.

[31] Goods SH, Brown LM. The nucleation of cavities by plastic deformation. Acta Metall 1979;27:1-15.
[32] McClintock FA. A Criterion for ductile fracture by the growth of holes. J Appl Mech 1968;35:363-71.
[33] Budiansky B, Hutchinson JW, Slutsky S. Void growth and collapse in viscous solids. In: Hopkins HG, Sewell MJ, editors. Mechanics of solids. Oxford: Pergamon Press; 1982.
[34] Ruggieri C, Panontin TL, Dodds R.,H. Numerical modeling of ductile crack growth in 3-D using computational cell elements. Int J Fract 1996;82:67-95.
[35] Thomason PF. Ductile fracture of metals. Oxford: Pergamon Press; 1990.
[36] Farrugia D. TATA Steel technical presentation. TATA Steel; 2012.
[37] Zhou W, Zhang R, Ai S, He R, Pei Y, Fang D. Load distribution in threads of porous metal–ceramic functionally graded composite joints subjected to thermomechanical loading. Compos Struct 2015;134:680-8.
[38] Afshan S, Balint D, Lin J, Farrugia D. Automated calibration of a void closure model for high-temperature deformation, J Multiscale Model 2011;3:79-90.
[39] Afshan S, Balint D, Lin J, Farrugia D. Micromechanical modelling of void healing, Adv Struct Mater 2013;19:1-8.
[40] Foster A. Ph.D Thesis. Birmingham: University of Birmingham; 2007.